

Cationic effects in polymer light-emitting electrochemical cells

Yufeng Hu and Jun Gao^{a)}

Department of Physics, Queen's University, Kingston, Ontario K7L 3N6, Canada

(Received 11 August 2006; accepted 21 November 2006; published online 22 December 2006)

The authors show that the emission zone position in a polymer light-emitting electrochemical cell (LEC) can be dramatically shifted by varying the monovalent cations used in the polymer electrolyte. A narrow light-emitting *p-n* junction very close to the center of the device has been imaged in planar LECs made with rubidium or cesium perchlorate, as compared to a more off-centered emission zone observed in LECs using other alkali perchlorates. In addition, LECs with a more centered emission zone display higher electroluminescence efficiency and better current stability. The authors attribute this effect to that of the cation size and mass, which affects the ionic mobility and doping propagation speed. © 2006 American Institute of Physics.

[DOI: 10.1063/1.2422877]

Polymer light-emitting electrochemical cells (LECs) are solid-state polymer light-emitting devices, in which the active material is an interpenetrating network of luminescent polymer and polymer electrolyte.¹⁻³ The operation of a LEC involves *in situ* electrochemical doping of the luminescent polymer and the formation of a light-emitting *p-n* junction.⁴ Electrochemical doping occurs when the reduction (or oxidation) of the luminescent polymer, achieved by the injection of electrons (or holes), is accompanied by the redistribution of counterions in the polymer electrolyte and their insertion between the reduced (or oxidized) polymer chains to compensate for the injected electronic charges.⁵ As a result of doping, the LEC operation is generally insensitive to the choice of electrode materials and the thickness of active layer. This is evidenced by the early demonstration and imaging of microplanar LECs with symmetric electrodes,^{1,6,7} and the recent demonstration of planar LECs with an extremely large interelectrode spacing of up to 11 mm.⁸⁻¹¹ Time-lapse fluorescence imaging of the millimeter-scale planar LECs enables us to visualize the entire LEC operating process with great spatial and temporal resolution.⁹⁻¹¹

An interesting observation is that the narrow light-emitting *p-n* junction (emission zone) formed is typically off centered.^{1,6-14} This phenomenon was initially explained in terms of a mobility asymmetry between electrons and holes in the luminescent polymer.^{7,15} However, high resolution time-lapse fluorescence imaging reveals that the direct cause of an off-centered emission zone in a LEC is the dissimilar *p*- and *n*-doping propagation speeds.¹¹ The electrochemical doping of the luminescent polymer, as manifested by the strong photoluminescence (PL) quenching, is always seen to originate from the electrode/polymer interfaces. Only when a *p-n* junction is formed by the initial contact of the *p*- and *n*-doped regions can electroluminescence (EL) be observed. A faster propagating *p* doping relative to *n* doping gives rise to an *initial* emission zone position closer to the negatively biased cathode, as seen in hundreds of millimeter-scale planar LECs we have imaged so far. It should be noted that in some microplanar LECs the light-emitting junction is seen to be closer to the anode.^{1,6,7} Further, the emission zone can shift across the center of the device to the cathode side dur-

ing continuous operation.⁴ Unfortunately, the fast dynamics of microplanar LECs precluded the determination of the initial emission zone position by the technique of time-lapse fluorescence imaging in these early studies.

Time-lapse fluorescence imaging enables us to identify many factors that affect the electrochemical doping and light emission processes in a LEC. These include, for example, the type of the luminescent polymer, voltage bias, operating temperature,^{8,16} and salt concentration.¹⁷ Since doping is achieved by the redistribution and insertion of counterions, we also expect the salt type, and therefore the properties of the mobile ions, to play an important role in the LEC processes. Indeed it has been shown that the choice of anions significantly affects the efficiency, kinetics, and stability of sandwich LECs made with lithium salts.^{18,19} In addition, we have recently observed that the certain cations (Eu³⁺ and Ag⁺) have strong effects on the doping and EL characteristics of LECs.^{11,20} Here we demonstrate planar and sandwich LECs made with various alkali perchlorate salts. We show that by varying the cations we can control the emission zone position in a LEC, which significantly affects the efficiency and stability of the devices.

All planar and sandwich LECs in this study utilized poly[5-(2'-ethylhexyloxy)-2-methoxy-1, 4-phenylene vinylene] (MEH-PPV) as the luminescent polymer. The polymer electrolyte consists of an ion-solvating polymer, poly(ethylene oxide) (PEO) ($M_n=100$ K), and an alkali perchlorate salt XClO₄, where X=Li, Na, K, Rb, or Cs. Perchlorates are used as opposed to the most commonly used triflates due to the commercial availability of all five alkali salts mentioned above. This choice of anion is justified because ClO₄⁻ and CF₃SO₃⁻ are both large polyatomic anions suitable for polyether-type polymer electrolyte formation.²¹ In addition, it has been shown that LECs made with lithium perchlorate and lithium triflate show similar device performance.¹⁹ A MEH-PPV:PEO weight ratio of 1:1 and an ether oxygen: cation ratio of EO:X=26:1 are maintained in all devices. Details about the LEC fabrication, testing, and imaging can be found in our previous publications.⁸⁻¹¹

The photographs of five 11 mm planar LECs containing various alkali perchlorate salts are shown in Fig. 1. Before any voltage bias was applied, the LEC films were highly photoluminescent due to the MEH-PPV content, as shown in

^{a)}Electronic mail: jungao@physics.queensu.ca

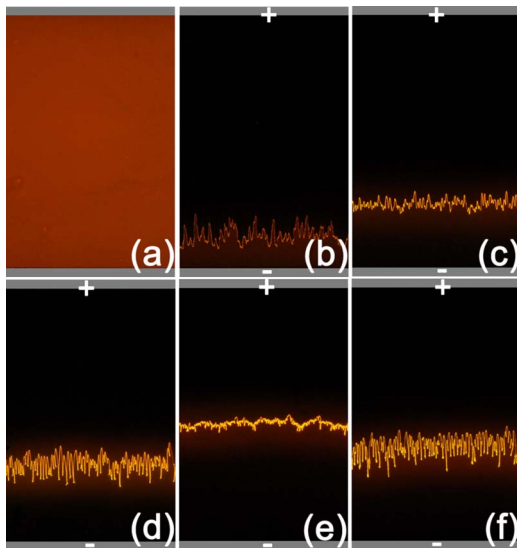


FIG. 1. (Color online) Photographs of Al/MEH-PPV:PEO:XCIO₄/Al planar LECs with an interelectrode spacing of 11 mm at their maximum EL. The devices are driven by an 800 V bias at a temperature of 340 K and imaged under UV illumination with a shutter speed of 2 s and an aperture of $f/14$. (a) $X=Li$, image taken before the application of the voltage bias; type of cation and time elapsed since the application of the voltage bias: (b) $X=Li$, 105 s; (c) $X=Na$, 70 s; (d) $X=K$, 154 s; (e) $X=Rb$, 322 s; and (f) $X=Cs$, 175 s. The polarity of voltage bias are labeled on the electrodes, which are marked by grey bars for clarity.

Fig. 1(a). An 800 V bias was then applied to turn on the devices at 340 K. Due to the extremely large interelectrode spacing of these devices, it typically takes minutes before the maximum EL is reached, which is preceded by doping propagation and p - n junction formation. Figures 1(b)–1(f) are photographs of all five MEH-PPV:PEO:XCIO₄ LECs near peak EL. Heavy PL quenching in both p - and n -doped regions renders the polymer film black when imaged under weak UV illumination. On the other hand, a narrow and highly uneven EL emission zone is clearly visible even with a naked eye in a dark room. Remarkably, the emission zone shifts significantly towards the device center with increasing cation size, with that of the Rb⁺ containing LEC being very close to the exact center of the device. Similar emission zone shift has also been observed in five planar LECs made from the same solutions, but with a 2 mm interelectrode spacing.

The average emission zone position for each of the devices, as measured from the anode, is extracted from the above images using a MATLAB program, and plotted against the ionic radii of the cations. Also shown in Fig. 2 are average positions of initially formed junctions. This second set of data is a more accurate measure of the relative p - and n -doping propagation speeds due to the drift of emission zone after its initial formation. The emission zone drift is negligible for Na⁺, K⁺, and Cs⁺ containing devices, but quite pronounced for Li⁺ and Rb⁺-based devices. The drift toward anode following the initial junction formation gives the Rb⁺-based LEC a more centered emission than the Cs⁺-based LEC. However, both sets of data show a similar trend: the emission zone position shifts toward the anode with increasing cation size. Especially when the junction is initially formed, the junction-to-cathode distance increases monotonically with cation size. Fluorescence imaging shows that the emission zone drift in Li⁺- and Rb⁺-based LECs is caused by a relative change in p - and n -doping volumes (area) after the

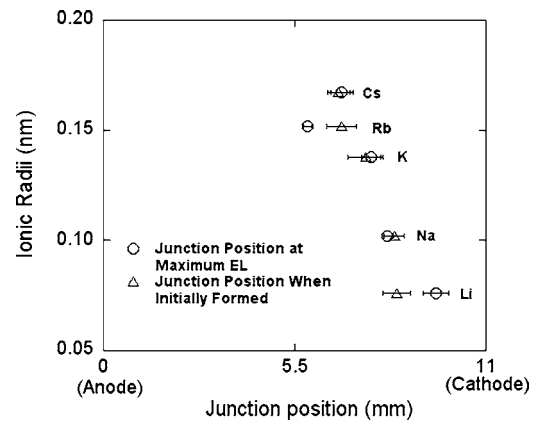


FIG. 2. EL emission zone position vs cation radius for the same devices when exhibiting maximum EL and when the light-emitting junction is initially formed.

junction is initially formed. The emission zone drift is negligible after maximum EL is reached.

A more centered emission zone is generally preferred over an off-centered one in polymer light-emitting devices due to reduced probability of exciton quenching by the metal electrodes. This is especially true for sandwich devices with a submicron interelectrode spacing and a large contact area between the electrodes and the active layer. To study possible cationic effects on LEC performance we have fabricated five sandwich LECs using the same solutions that were used to make the planar LECs. Figure 3 displays EL efficiency versus current characteristics (a) and the time evolution of device current (b) in all five devices. Devices made with larger cations display higher peak efficiency, which is highest in the Cs⁺-based device. In addition, Cs⁺-, Rb⁺-, and K⁺-based devices display much better current stability than Li⁺- and Na⁺-based devices under a constant driving voltage of 3 V.

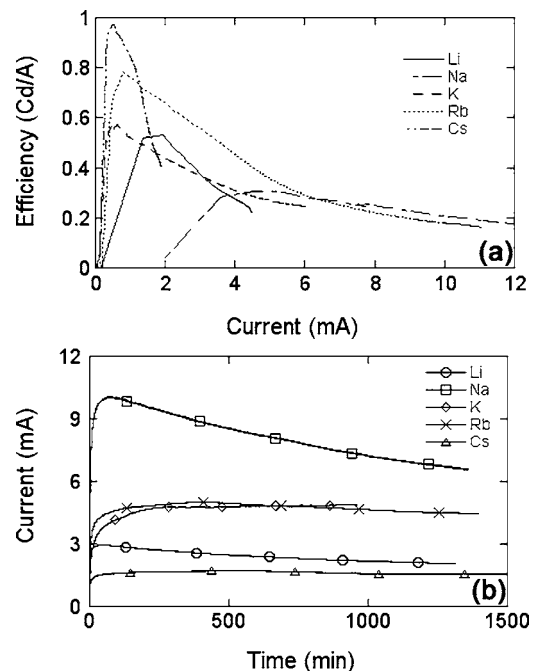


FIG. 3. EL efficiency vs current (a) and device current vs time (b) characteristics for sandwich LECs made with various alkali perchlorates XCIO₄ ($X=Li, Na, K, Rb, Cs$) under a constant bias of 3 V at room temperature. The devices are made on indium tin oxide coated glass substrate with $2 \times 6 \text{ mm}^2$ Al top contact.

TABLE I. Doping propagation speeds and area ratios of *p*- and *n*-doped regions for 11 mm planar LECs made with various alkali perchlorates

Cation [radius (nm)]	v_p doping (mm/s)	V_n doping (mm/s)	V_p doping/ V_n doping	A_p/A_n
Li ⁺ (0.060)	0.122	0.037	3.30	3.29
Na ⁺ (0.095)	0.394	0.101	3.90	3.17
K ⁺ (0.133)	0.236	0.093	2.54	2.17
Rb ⁺ (0.148)	0.180	0.098	1.84	1.64
Cs ⁺ (0.169)	0.167	0.096	1.74	1.59

We believe that the cationic effect described above is most likely caused by a systematic change in cation mobility, which affects the doping propagation speed and therefore the junction position. The alkali cations used in this study are all monovalent and similar in their complex formation ability with ether oxygen, but differ significantly in size and mass.²² Both the mass and the size of the cation affect its mobility. The cation transport in a polymer electrolyte strongly depends on the creation of “free volume” that the ions can migrate into. This explains the size dependence of cation mobility. Although *p*-doping is achieved by the insertion of anions between oxidized luminescent polymer units, the *p*-doping propagation speed is actually determined by the mobility of cations, which must migrate away from the anode region for *p* doping to occur, and vice versa for *n* doping. This assumption is supported by our earlier calculation of cation (Li⁺) mobility based on the propagation speed of *p*-doping frontier.¹⁶ In these LECs based on alkali perchlorates, we expect the *n*-doping propagation speed to be invariant because the same ClO₄⁻ anion is involved in all devices. On the other hand, the *p*-doping propagation speed should decrease with increasing cation size due to decreasing cation mobility. This prediction is supported by the data shown in Table I. *p*- and *n*-doping propagation speeds were extracted from consecutive fluorescent images of the devices during the turn on process based on a technique we developed earlier.¹⁶ Also included in Table I are ratios of *p*- and *n*-doping propagation speeds (v_p/v_n) and the area ratios of *p*- and *n*-doped regions (A_p/A_n) when the junction is initially formed. As expected, the two ratios are close and show the same trend with increasing cation size. We therefore can draw the conclusion that more balanced cation and anion mobilities lead to a more centered emission zone. We also note that the doping speeds in Li⁺-based LECs are anomalously low. This is likely due to the formation of ion pairs or aggregates with reduced mobilities or incomplete solvation of the LiClO₄ salt. These effects are expected to become less dominant as the center-to-center distance between cation and anion increases with cation size.

In summary, we have studied the effects of varying alkali cations on the emission zone position and performance

of LECs. The systematic shift in emission zone position towards the device center with increasing cation size/mass is interpreted in terms of cation mobility change, which affects *p*-doping propagation speed. A more centered emission zone is obtained in LECs made with the largest cations, which also display better device performance.

The authors thank the American Dye Source, Inc. for providing the luminescent materials used in this work. The research is supported by the Natural Sciences and Engineering Research Council of Canada.

¹Q. B. Pei, G. Yu, C. Zhang, Y. Yang, and A. J. Heeger, *Science* **269**, 1086 (1995).

²Y. Cao, G. Yu, A. J. Heeger, and C. Y. Yang, *Appl. Phys. Lett.* **68**, 3218 (1996).

³L. F. Santos, L. M. Carvalho, F. E. G. Guimaraes, D. Goncalves, and R. M. Faria, *Synth. Met.* **121**, 1697 (2001).

⁴Q. B. Pei, Y. Yang, G. Yu, C. Zhang, and A. J. Heeger, *J. Am. Chem. Soc.* **118**, 3922 (1996).

⁵B. Scrosati, in *Solid State Electrochemistry*, edited by P. G. Bruce (Cambridge University Press, Cambridge, UK, 1995), p. 234.

⁶D. J. Dick, A. J. Heeger, Y. Yang, and Q. B. Pei, *Adv. Mater. (Weinheim, Ger.)* **8**, 985 (1996).

⁷Y. Yang and Q. B. Pei, *Appl. Phys. Lett.* **68**, 2708 (1996).

⁸J. Gao and J. Dane, *Appl. Phys. Lett.* **83**, 3027 (2003).

⁹J. Gao and J. Dane, *Appl. Phys. Lett.* **84**, 2778 (2004).

¹⁰J. Gao and J. Dane, *J. Appl. Phys.* **98**, 063513 (2005).

¹¹Y. Hu, C. Tracy, and J. Gao, *Appl. Phys. Lett.* **88**, 123507 (2006).

¹²J. M. Leger, S. A. Carter, and B. Ruhstaller, *J. Appl. Phys.* **98**, 124907 (2005).

¹³J. H. Shin, A. Dzwilewski, A. Iwasiewicz, S. Xiao, A. Fransson, G. N. Ankah, and L. Edman, *Appl. Phys. Lett.* **89**, 013509 (2006).

¹⁴L. Edman, M. A. Summers, S. K. Buratto, and A. J. Heeger, *Phys. Rev. B* **70**, 115212 (2004).

¹⁵J. A. Manzanares, H. Reiss, and A. J. Heeger, *J. Phys. Chem. B* **102**, 4327 (1998).

¹⁶J. Dane, C. Tracy, and J. Gao, *Appl. Phys. Lett.* **86**, 153509 (2005).

¹⁷Y. Zhang, C. Tracy, and J. Gao (unpublished).

¹⁸L. Edman, D. Moses, and A. J. Heeger, *Synth. Met.* **138**, 441 (2003).

¹⁹Y. Cao, Q. B. Pei, M. R. Andersson, G. Yu, and A. J. Heeger, *J. Electrochem. Soc.* **144**, L317 (1997).

²⁰Y. Hu, Y. Zhang, and J. Gao, *Adv. Mater. (Weinheim, Ger.)* **18**, 2880 (2006).

²¹F. M. Gray, *Polymer Electrolytes* (The Royal Society of Chemistry, Cambridge, UK, 1997), p. 12.

²²F. M. Gray, *Solid Polymer Electrolytes: Fundamentals and Technological Applications* (VCH, New York, 1999), p. 49.